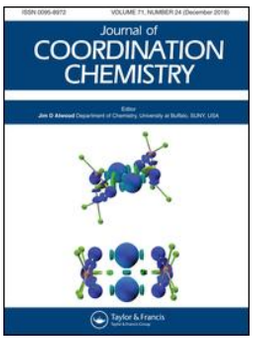

Taylor & Francis
Taylor & Francis Group

Journal of Coordination Chemistry

ISSN: 0095-8972 (Print) 1029-0389 (Online) Journal homepage: https://www.tandfonline.com/loi/gcoo20

New bioactive Cu(I) thiourea derivatives with triphenylphosphine; synthesis, structure and molecular docking studies

Shazia Hussain, Imtiaz-ud-Din, Ahmad Raheel, Shabeeb Hussain, Muhammad Nawaz Tahir & Irfan Hussain

To cite this article: Shazia Hussain, Imtiaz-ud-Din, Ahmad Raheel, Shabeeb Hussain, Muhammad Nawaz Tahir & Irfan Hussain (2020): New bioactive Cu(I) thiourea derivatives with triphenylphosphine; synthesis, structure and molecular docking studies, Journal of Coordination Chemistry, DOI: 10.1080/00958972.2020.1771558

To link to this article: https://doi.org/10.1080/00958972.2020.1771558

JOURNAL OF COORDINATION CHEMISTRY
https://doi.org/10.1080/00958972.2020.1771558

Taylor & Francis
Taylor & Francis Group

New bioactive Cu(I) thiourea derivatives with triphenylphosphine; synthesis, structure and molecular docking studies

Shazia Hussain[a], Imtiaz-ud-Din[a], Ahmad Raheel[a], Shabeeb Hussain[a], Muhammad Nawaz Tahir[b] and Irfan Hussain[c]

[a]Department of Chemistry, Quaid-i-Azam University, Islamabad, Pakistan; [b]Department of Physics, University of Sargodha, Sargodha, Pakistan; [c]Department of Biotechnology, Quaid-i-Azam University, Islamabad, Pakistan

ABSTRACT

The synthesized thioureas, 1-(3-fluorobenzoyl))-3-(4-(diethyl aminophenyl) thiourea ($\mathbf{l_1}$), 1-benzoyl-3-(2-chlorophenyl) thiourea ($\mathbf{l_2}$) and 1-(2-fluorobenzoyl)-3-(2-chlorophenyl) thiourea ($\mathbf{l_3}$) along with triphenylphosphine were reacted with Cu(I) chloride in mole ratios 1:2:1 by using dry acetone as solvent under nitrogen to get **1**–**3**. The synthesized thioureas and metal derivatives were characterized by spectroscopic techniques such as IR and multinuclear (^{1}H, ^{13}C) NMR. Compound **3** is analyzed by single crystal X-ray analysis and data reveal that the Cu is four coordinate having tetrahedral molecular geometry. The interaction of **1**–**3** with DNA is ascertained by cyclic voltammetry, determining binding constant, binding energy and diffusion coefficient. The findings suggest that the complexes interact with DNA in an electrostatic mode. The antioxidant activity data show that **3** has the highest free radical scavenging ability having Ic_{50} value of 10 µg/mL. The synthesized compounds were also screened against various bacterial strains and found some encouraging results. The binding interactions of the metal complexes with a specific protein were further validated by molecular docking studies and the results obtained show their strong interaction with amino acid residue in the binding pocket of the target protein.

ARTICLE HISTORY
Received 21 September 2019
Accepted 29 April 2020

KEYWORDS
Copper; thioureas; triphenylphosphine; antioxidant; antimicrobial; DNA binding

CONTACT Imtiaz-ud-Din drimtiazuddin@Yahoo.com Department of Chemistry, Quaid-i-Azam University, Islamabad 45320, Pakistan.

Supplemental data for this article is available online at https://doi.org/10.1080/00958972.2020.1771558.

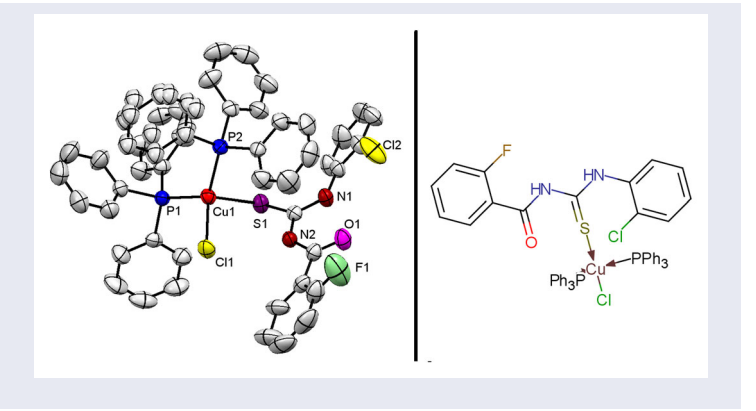

1. Introduction

Compounds having carbonyl and thiocarbonyl functionalities behave as versatile donor ligands for transition metal ions [1–7]. Derivatives of thiourea are well known for their intra- and intermolecular hydrogen bonding capabilities. They are also used as important ligands in coordination chemistry with potential to coordinate with various metal ions as mono or dianions, or as neutral ligands [8–12]. Thioureas with these added properties are used in self-assembled network materials [13]. The nitrogen, sulfur and oxygen donors of thioureas and their derivatives provide various possibilities to coordinate with transition metal ions to yield useful chemical products. Thioureas as well as their metal complexes have been screened for a variety of biological activities and are important because of their special role in biological systems [14–17]. Some thiourea derivatives have also been used as fungicides on a commercial scale [18–22].

Among trace metals, copper plays an important role in the development and performance of nerve, cardiovascular, immune and reproductive systems besides the nourishment of skin, bones as well as gene transcription of humans [23–26]. Copper forms a wide range of coordination complexes in both I and II oxidation states; copper(III) complexes have been rarely reported [27]. In comparison to Cu(II) coordination compounds of Cu(I) are less common but are more interesting in terms of their structural and biological aspects. Complexes of copper(I/II) are less structurally predictable as compared to other first row transition metal complexes as they are labile, redox active and frequently have distorted coordination geometries. Cu(I) ions prefer ligands having soft donors like S and P, besides their strong interaction with thioethers and aromatic amines. Although three-coordinate trigonal and two-coordinate linear arrangements for Cu(I) complexes are known, four-coordinate tetrahedral geometry is more common; Cu(II) complexes exhibit coordination numbers ranging from four to six with square-planar, trigonal bipyramidal and octahedral geometries [28]. The redox potential of Cu(I/II) couples varies dramatically with changing ligand environment, steric/chelating effect and geometry of the complexes [29].

Reports indicate that both thiourea and derivatives with copper exhibit significant role in biological activities such as antifungal, antihelmintic, herbicidal, antitubercular,

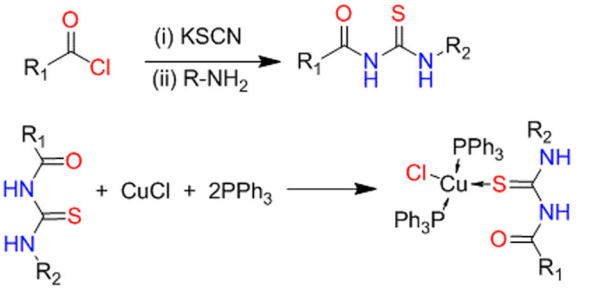

	R_1	R_2
I_a, 1	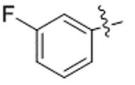	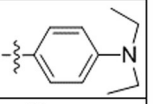
I_b, 2	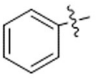	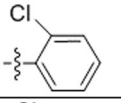
I_c, 3	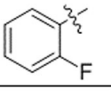	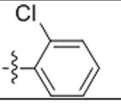

Scheme 1. Synthesis of the thioureas, I_1-I_3 (a) and of Cu(I) complexes, **1**-**3** (b).

antibacterial, antithyroid, insecticidal and rodenticide [30–34]. Several series of copper(I) complexes with N,N′-disubstituted thiourea ligands have been synthesized, characterized and screened for possible roles as antimicrobial agents [35, 36]. They were also found to serve as active catalysts for oxidation of primary and secondary alcohols [37]. Keeping in view the homological significance of the copper species and in continuation of our previous work [38–42], we report herein some new substituted thioureas and their Cu(I) complexes using triphenylphosphine as a ligand. The focus of the present study is the syntheses of compounds that could enhance the hydrophilicity/hydrophobicity of such drug candidates by introducing various substituents in their structural motifs.

2. Experimental

2.1. Materials and methods

Benzoyl chloride, 2-fluorobenzoyl chloride, 3-fluorobenzoyl chloride, potassium thiocyanate, 2-chloroaniline, N,N-diethyl-1,4-phenylenediamine, triphenylphosphine and copper(I) chloride were purchased from Sigma-Aldrich (USA) and used as received.

2.2. Synthesis

The general methodology used for synthesis of thiourea derivatives (**I_1**–**I_3**) and their metal complexes (**1**–**3**) are depicted in scheme 1, the details of which may be summarized as follows:

Stoichiometric amounts of substituted benzoyl chlorides and potassium thiocyanate were stirred for one hour, subsequently, the respective amines were added. The mixture was stirred for another 4 h to get the desired thiourea derivatives (**I_1–I_3**). The completion of the reaction was monitored through TLC and the reaction mixture was poured into ice cooled distilled water. The resultant dark green product precipitated out, was washed with water and dried in air.

Subsequently the synthesized thioureas and triphenylphosphine were complexed with Cu(I) salt to yield **1**–**3**. For that, 0.099 g (1 mmol) Cu(I)Cl, 0.52 g (2 mmol) triphenylphosphine and (1 mmol) of the respective thiourea were dissolved separately in ethanol. Then solutions of triphenylphosphine and the respective thiourea were added simultaneously into the solution of Cu(I) halide and stirred for 4–5 h. The solid product precipitated out, was filtered and dried at room temperature. The compounds were recrystallized in a mixture of acetone/ethanol (1:3) to get pure products, however, suitable crystals for only **3** could be obtained for X-ray diffraction analysis.

2.2.1. 1-(3-Fluorobenzoyl)-3-(4-(diethylamino) phenyl) thiourea (I_1)

Quantities used were: 1.58 mL (15 mmol) 3-fluorobenzoyl chloride, 1.44 g (15 mmol) potassium thiocyanate and 2.49 mL (15 mmol) N,N-diethyl-1,4-phenylenediamine. Yield: 94%. m.p. 129–131 °C. IR data (υ, cm^{-1}); NH (3419), C = O (1663), C = S (1196), C = C Ar (1518), CH_{sp2} (3047). ^{1}H NMR data ($CDCl_3$, δ, ppm): 12.2 (s, 1H, CSNH), 9.2 (s, 1H, CONH), 7.6-6.6 (m, 8H Ar), 3.4 (q, 4H, 2(-CH_2-)), 1.2 (t, 6H, 2(-CH_3)). ^{13}C NMR data ($CDCl_3$, δ, ppm): 177.3, 165.6, 164.4 146.7, 134.1 130.9 125.5, 122.9, 120.7, 120.4, 115.2, 114.9, 111.3, 44.4, 12.5.

2.2.2. 1-Benzoyl-3-(2-chlorophenyl) thiourea (I_2)

Quantities used were: 2.32 mL (20 mmol) benzoyl chloride, 1.92 g (20 mmol) potassium thiocyanate and 2.5 mL (20 mmol) 2-chloroanilne. Yield: 93%; m.p: 130–132 °C. IR data (υ, cm^{-1}); NH (3318), C = O (1665), C = S (1210), C = C Ar (1516), CH_{sp2} (3035). ^{1}H NMR data ($CDCl_3$, δ, ppm): 12.7(s, 1H, CSNH), 9.3 (s, 1H, CONH), 7.2-6.3 (m, 9H, aromatic). ^{13}C NMR data ($CDCl_3$, δ, ppm): 178.7, 165.6, 164.2, 160.9, 135.6, 134.4, 133.5, 130.8, 128.7, 126.9, 126.1, 125.4, 124.6, 122.1, 120.8, 116.1, 115.8.

2.2.3. 1-(2-Fluorobenzoyl)-3-(2-chlorophenyl)thiourea (I_3)

Quantities used were: 3.47 mL (30 mmol) 2-fluorobenzoyl chloride, 2.88 g (30 mmol) potassium thiocyanate and 3.5 mL (30 mmol) 2-chloroaniline. Yield: 93%, m.p: 140–142 °C. IR data (υ, cm^{-1}); NH (3414), C = O (1673.5), C = S (1202), C = C Ar (1525), CH_{sp2} (3057). ^{1}H NMR data ($CDCl_3$, δ, ppm): 12.71 (s, 1H, CSNH), 9.1 (s, 1H, CONH), 8.4-7.7 (m, 8H Ar). ^{13}C NMR data ($CDCl_3$, δ, ppm): 178.4, 16.8, 16.2, 136.2, 135, 132.3, 129.6, 127.9, 127.7, 126.9, 126.1, 125.4, 116.9, 116.6.

2.2.4. Bis-(triphenylphosphine)-1-(3-fluorobenzoyl)-3-(4-(diethylamino)phenyl) thioureacopper(I) chloride (1)

The quantities were: 0.69 g (1 mmol) 1-(4-(diethyl amino)phenyl)-3-(3-fluorobenzoyl) thiourea, 0.52 g (2 mmol) triphenylphosphine and 0.099 g (1 mmol) CuCl. Yield: 91%, m.p: 173–175 °C. IR data (υ, cm^{-1}); NH (3422), C = O (1662), C = S (1152), C = C Ar

(1521), sp^2 CH (3047). ^{1}H NMR data ($CDCl_3$, δ, ppm): 12.3 (s, 1H, CSNH), 10.4 (s, 1H, CONH), 7.9-6.6 (m, 38H, Ar), 3.4 (q, 4H, NC_4H_{10}), 1.2 (t, 6H, NC_4H_{10}). ^{13}C NMR data ($CDCl_3$, δ, ppm): 176.9, 166.6, 164.3 ($J = 247.5$ Hz), 146.70, 134.5, 134.1 133.5, 130.6, 129.2, 128.4, 125.8, 125.09, 124.3, 120.7, 120.5, 115.9, 115.6, 111.1, 29.2, 12.5.

2.2.5. Bis-(triphenylphosphine)1-benzoyl-3-(2-chlorophenyl)thiourea)copper(I) chloride (2)

Quantities used were: 0.493 g (1 mmol) 1-benzoyl-3-(2-chlorophenyl) thiourea, 0.52 g (2 mmol) triphenylphosphine and 0.099 g (1 mmol) CuCl. Yield: 92%, m.p: 190–193 °C. IR data (υ, cm^{-1}); NH (3421), C = O (1669), C = S (1157), C = C Ar (1519), sp^2 CH (3034.5). ^{1}H NMR data ($CDCl_3$, δ, ppm): 12.6 (s, 1H, CSNH), 11.0 (s, 1H, CON), 7.2-6.3 (m, 39H, aromatic), ^{13}C NMR data ($CDCl_3$, δ, ppm): 178.6, 168.9, 164.4, 161.0, 135.7, 134.6, 133.4, 130.9, 128.6, 127.0, 126.2, 125.5, 124.6, 122.2, 120.7, 116.3, 115.9.

2.2.6. Bis-(triphenylphosphine)1-(2-fluorobenzoyl)-3-(2-chlorophenyl)thiourea Cu(I) chloride (3)

Quantities used were: 0.617 g (1 mmol) 1-(2-fluorobenzoyl)-3-(2-chlorophenyl) thiourea, 0.52 g (2 mmol) triphenylphosphine and 0.099 g (1 mmol) CuCl. Yield: 90%, m.p: 173–175 °C. IR data (υ, cm^{-1}); NH (3425), C = O (1677), C = S (1150), C = C Ar (1528), CH_{sp2} (3057). ^{1}H NMR data ($CDCl_3$, δ, ppm): 12.7 (s, 1H, CSNH), 11.2(s, 1H, CONH), 8.3-7.1 (m, 38H Ar). ^{13}C NMR data ($CDCl_3$, δ, ppm): 178.9, 165.6, 162.37, 135.2, 134.68, 134.0, 133.3, 133.0, 131.7, 129.7, 129.6, 128.5, 127.9, 127.0, 126.8, 124.7, 116.7, 116.4.

2.3. Cyclic voltammetry and DNA binding studies

Interactions of **1**–**3** with CT-DNA were determined by using Eco Chemie Auto lab PGSTAT 12 potentiostat/galvanostat (Utrecht, The Netherlands), which consists of a three electrode system in which platinum disc was used as working electrode, Ag/AgCl as reference electrode and platinum wire as counter electrode. The working electrode was washed with acetone and doubly distilled water before use. The cyclic voltammograms were recorded between −0.5 to 1.25 volts at scan rate of 100–700 mVs^{-1} to probe the nature of electrochemical process occurring at the electrode surface and the binding affinity of **1**–**3** with CT-DNA.

2.4. Antioxidant activity

Solution of DPPH was prepared in dry ethanol and 2 ml was mixed with 2 ml ethanolic solution of **1**–**3** having different concentrations (3.12, 6.25, 12.50, 25, 50 100, 200 and 400 μM) in the test tubes. In one test tube, 2 ml of DPPH solution was mixed with 2 ml of ethanol which is taken as drug free solution serving as the reference. The resultant solutions were kept in the dark for thirty minutes and then their absorption spectra were recorded by UV-visible spectroscopy.

2.5. Antibacterial activity

Three pathogen bacteria were employed as test organisms, *E. coli*, *Pseudomonas* and *Staphylococcus aureus*. Sterile discs (Oxoid) were soaked with 50 µl of each methanolic solution of the compound at a concentration of 200 µg/ml and 400 µg/ml and then dried. These discs were placed on Mueller-Hinton agar plates, previously swabbed with the target bacterial isolate at a concentration of 106 CFU/ml in one disc; the respective organic solvent was added as negative control and the commercially available antibiotic drug, erythromycin, as a positive control to determine the possible inhibitory activity of the solvent and for corroborative evidence. The preparation was incubated for 24 h at 37 °C and antibacterial activity has been defined as the diameter (mm) of the clear inhibitory zone formed around the discs.

2.6. Molecular docking study

Autodock was used to perform the docking simulations employing the 3D structure of *E.coli enoyl reductase* (PDB code: 1C14). The Protein Data Bank was used to retrieve the "pdb" file (www.pdb.org). After removal of all heteroatoms and the ligand, the Autodock tools were used to convert the protein to pdbqt format (1.5.6) [43]. For the preparation of ligand, the Marvin sketch (5.8.3) was used for two-dimensional chemical structures of ligands (http://www.chemaxon.com) and these structures were converted to 3D format by Open Babel (ver. 2.3.1) [44]. Finally, an Autodock Tool was used to prepare the final pdbqt format of ligands. The following parameters were used to perform the docking simulation: size $x = 73.91$; size $y = 63.29$; size $z = 53.03$ center $x = -1.7242$; center $y = 32.18$; center $z = 145.550$.

3. Results and discussion

Three new Cu(I) complexes (**1**–**3**) were prepared by reacting the respective substituted thioureas (**I_1**–**I_3**) with Cu(I) chloride with triphenylphosphine as a second ligand through the methodology delineated in Scheme 1. **1**–**3** are quite stable in moist air and soluble in common organic solvents. The synthesized compounds were characterized by IR and multinuclear (^{1}H and ^{13}C) spectroscopy and complete data are presented in the experimental section. Complex **3** has also been characterized by single crystal XRD to authenticate its structure.

3.1. Spectroscopic studies

The FT-IR data show a broad band from 3450 to 3250 cm^{-1} indicating the presence of NH group and its broadening is because of the existence of intermolecular and intramolecular hydrogen bonds in the structural motif of **1**–**3**, confirmed by the X-ray crystallographic data for **3**. The carbonyl and thiocarbonyl groups have characteristic bands at 1700–1650 and 1250–1130 cm^{-1}, respectively [45]. The IR absorption band for (C = S) functionality appears around 1200 cm^{-1} in the ligand and a slight frequency shift was found at around 1156 cm^{-1} in the complexes, which demonstrate that coordination occurred through sulfur of the thiourea moiety for **1**–**3**. A stretch at 1080 cm^{-1}

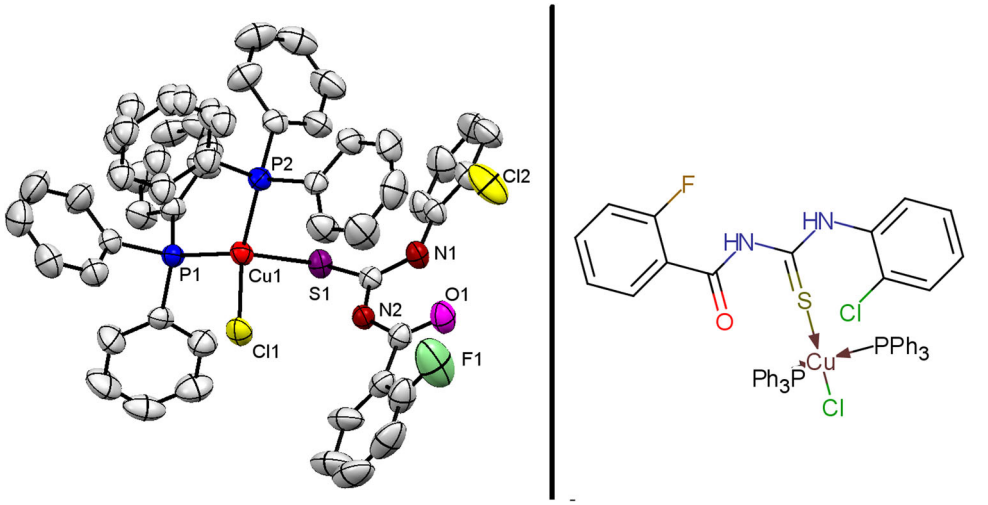

Figure 1. ORTEP diagram and molecular structure for **3** drawn at 50% probability.

may be assigned to P–C_{Ph} which clearly demonstrates the linkage of PPh_3 to the Cu(I) thiourea system [36].

^{1}H NMR data show the NH, present between the carbonyl and thionyl group in **1**–**3**, at 9.1–9.3 ppm whereas the other NH proton resonates at 12.3–12.7 ppm [36, 38]. The NH proton which is not between the carbonyl and thiocarbonyl group is more de-shielded due to its intermolecular hydrogen bonding with the carbonyl group of the other molecule, confirmed by the crystallographic data (Figure 1).

All distinct carbons, present in **1**–**3**, have been explicitly resolved by ^{13}C NMR spectroscopic data. By comparing the chemical shift values, calculated from the incremental method, to experimental chemical shifts, the aromatic carbon resonances have been designated easily and the data are in agreement with reported values [45–47]. The aromatic carbons resonate at 120–135 ppm, whereas carbon of C = O and C = S resonate at 164–166 and 175–179 ppm, respectively, as earlier reports manifested [36].

3.2. X-ray crystallography

ORTEP diagram and molecular structure for **3** is given Figure 1 whereas crystal structure refinement details are given in Table 1. Selected bond distances and angles are listed in table S1 (as Supplementary Information). The crystal structure for **3** with general formula [$Cu(PPh_3)_2(L)$] shows that Cu is four coordinate with a distorted tetrahedral molecular geometry. The thiourea (1-(2-chlorophenyl)-3-(2-fluorobenzoyl) thiourea) coordinates to copper via S-donor and the binding is in a terminal mode. The two triphenylphosphine molecules are bound to phosphorus. The corresponding P–Cu–P angle is 115.59 while S–Cu–P angle varies from 102.56 to 105.51° and S–Cu–Cl angle transcends 102.83°. The torsional angles showed that thiocarbonyl moiety and carbonyl group are coplanar. The crystal structure analysis further described the existence of two independent molecules in a unit cell, connected through intermolecular C–H … Cl hydrogen bonding. The structural analysis further revealed that there exists two types of intramolecular hydrogen bonds between O_1 and hydrogen of N1

Table 1. Crystal data and structure refinement for **3**.

Empirical formula	$C_{50}H_{40}Cl_2CuFN_2OP_2S$
Formula weight	932.28
Temperature/K	296(2)
Crystal system	Triclinic
Space group	P-1
a/Å	11.5138(4)
b/Å	12.0528(4)
c/Å	18.0125(6)
α/°	90.715(2)
β/°	106.5080(10)
γ/°	111.170(2)
Volume/Å^3	2216.28(13)
Z	2
ρ_{calc}g/cm^3	1.397
μ/mm^{-1}	0.777
F(000)	960.0
Crystal size/mm^3	0.430 × 0.350 × 0.300
Radiation	MoKα ($\lambda = 0.71073$)
2Θ range for data collection/°	4.494–54
Index ranges	$-14 \leq h \leq 14$, $-15 \leq k \leq 15$, $-23 \leq l \leq 22$
Reflections collected	32390
Independent reflections	9605 [$R_{int} = 0.0262$, $R_{sigma} = 0.0252$]
Data / restraints / parameters	9605 / 0 / 512
Goodness-of-fit on F^2	1.020
Final *R* indices [$I \geq 2\sigma$ (*I*)]	$R_1 = 0.0426$, w$R_2 = 0.1112$
Final *R* indices [all data]	$R_1 = 0.0529$, w$R_2 = 0.1201$
Largest diff. peak/hole /e Å^{-3}	0.96 / −0.79

(O1 … .HN1) and Cl1 and hydrogen of N2 (Cl1. … HN2). Thus single crystal X-ray data demonstrate formation of the coordination compound via linkage of ligating atoms of the respective ligands with existence of intra- and intermolecular H-bonding that impart stability to the molecule (Figures 1 and 2).

3.3. DNA binding studies

The interactions of the compounds with CT-DNA were established with cyclic voltammetry. The voltammograms were recorded in the presence as well as in the absence of DNA at different scan rates for finding the electrochemical nature and binding affinity for **1**–**3** by using ethanol as solvent. The electrochemical behavior for **3** is discussed here in detail (Figures 3 and 4) whereas the cyclic voltammetric data for **1** and **2** are presented in Table 2. The potential region, which lies between −0.4 to 0.8 volts, has been selected to study the electrochemical nature of the process occurring at the electrode surface and to find the binding affinity of **1**-**3** with CT-DNA.

The cyclic voltammogram of **3** revealed the emergence of two oxidation peaks and one reduction peak from −0.4 to 0.8 volt (figure 3). The well-defined oxidation peak at 0.25 volt and reduction peak at −0.08 volt were selected for further insight into the interaction of **3** with CT-DNA and to find the nature of electrochemical process occurring at the working electrode. The current decreases after addition of DNA into the solution of **3** from formation of the adduct by which the molecule becomes heavier as it diffuses more slowly than the lighter one. The negative shift in the peak position describes the electrostatic mode of interaction between the compound and the phosphate backbone of CT-DNA [48]. The electrostatic mode of interaction between **3** and

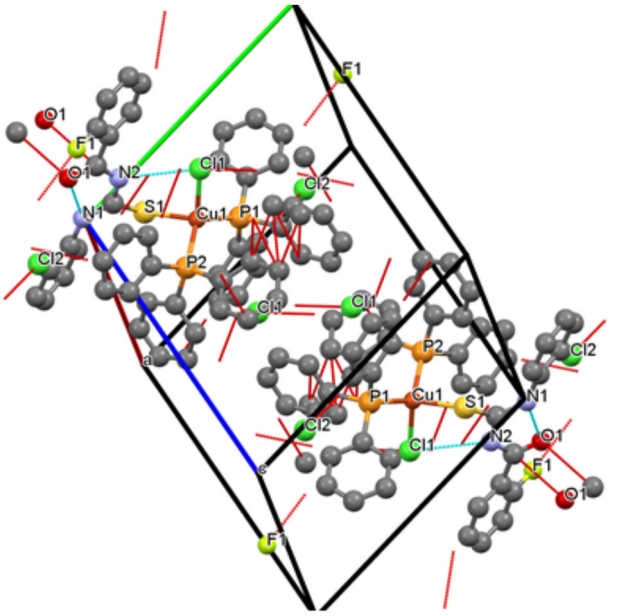

Figure 2. Packing diagram for **3** depicting intermolecular (C-H . . . .Cl) hydrogen bond and intramolecular hydrogen bonds (O1 . . . .HN1) and (Cl1. . . . HN2).

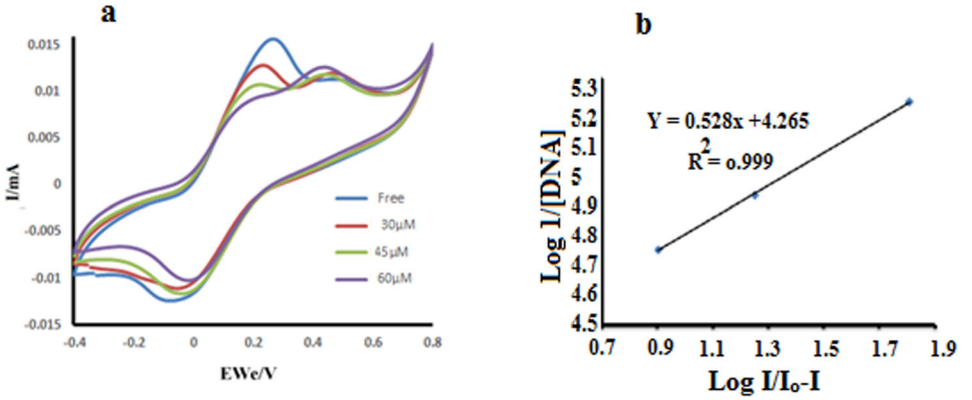

Figure 3. (A) Representative cyclic voltammogram for **3** of 1 mM concentration recorded at 100 mVs^{-1} and (B) Plot of Log $I/(I_o-I)$ vs. Log 1/[DNA] for **3**.

DNA may be ascribed to the copper whose presence provides the partial positive center and interact electrostatically with the phosphate backbone of the DNA double helix structure. The binding constants and binding energies for **1**–**3** were calculated from the plot, Log $I/(I_o-I)$ versus Log1/[DNA], as shown in Figure 3(A) where I_o represents the current observed at E_{pa} for the complex without DNA while I represents the current observed at E_{pa} after addition of DNA. The binding parameters are listed in table 2.

$$i_p = 2.69x10^5 n^{3/2} ACD^{1/2} \upsilon^{1/2} \quad (1)$$

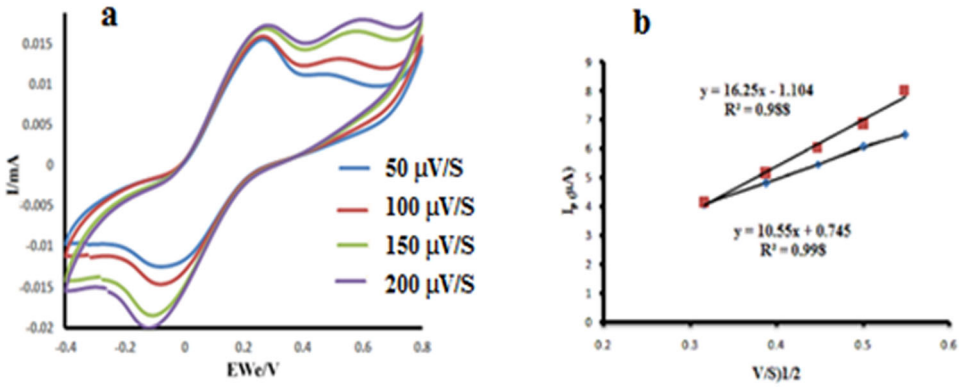

Figure 4. Cyclic voltammogram of 1 mM **3** at different scan rates (50–200 µV/s) at 298 K in alcoholic solution; supporting electrolyte 0.1 M TBAP (B) I_p vs. $\upsilon^{1/2}$ plots of 1 mM **3** in the absence of DNA (blue) and presence of 30 µM DNA (brown) at scan rates ranging from 50 to 200 mVs^{-1}.

Table 2. DNA Binding constants and binding energies for **1–3**.

Compounds	$\Delta E_p = E_{pa} - E_{pc}$	Binding constant (M^{-1})	Binding energy (kJM^{-1})	D_o [$cm^2\ s^{-1}$] free drug	D_o [$cm^2\ s^{-1}$] drug-DNA
1	0.38	8.19×103	22.33	2.93×10^{-5}	1.23×10^{-3}
2	0.35	5.65×103	21.41	9.87×10^{-3}	5.13×10^{-3}
3	0.33	5.31×103	15.54	7.23×10^{-3}	3.05×10^{-3}

$$E_{pa} - E_{pa}/2 = 47.7/\alpha_a n \quad (2)$$

The cyclic voltammograms of 1 mM complexes without CT-DNA at the scan rates 50, 100, 150 and 200 mVs^{-1} were recorded. Similarly, cyclic voltammograms at the scan rates 50, 100, 150 and 200 mVs^{-1} were taken after the addition of 30 µM CT-DNA. The non-consistency of the oxidation and reduction potential with changing scan rate and the ratio between the cathodic and anodic current is not unity could describe the quasi nature of electrochemical process occurring at the electrode surface. The diffusion coefficients of the DNA free complexes and of the complex-DNA adduct can be calculated from the plot of I_p vs. $\upsilon^{1/2}$ (Figure 4) by applying Equations (1) and (2), the values of which are given in Table 2. The data clearly demonstrate that decrease in values after adduct formation is because it is heavier and the adducts diffuse with slower rate than the DNA free samples.

3.4. Antioxidant activity

The ability of **1–3** to scavenge the free radicals were evaluated by 1,1-diphenyl-2-picryl-hydrazyl (DPPH) assay in ethanol. There is a decrease in absorbance at 517 nm of DPPH solution as the concentration of the added compound increases from 1.56 to 25 uM (Figure 5). The data, thus, show that the added compounds have the ability to scavenge the DPPH free radicals as there is a decrease in absorbance as a result of reduction in concentration of free radicals. The decrease in absorbance of DPPH at 517 nm has been used to find the antioxidant activity of chemical compounds [32]. The ascorbic acid was used as standard and found to have IC_{50} value of 12.1 µg/mL.

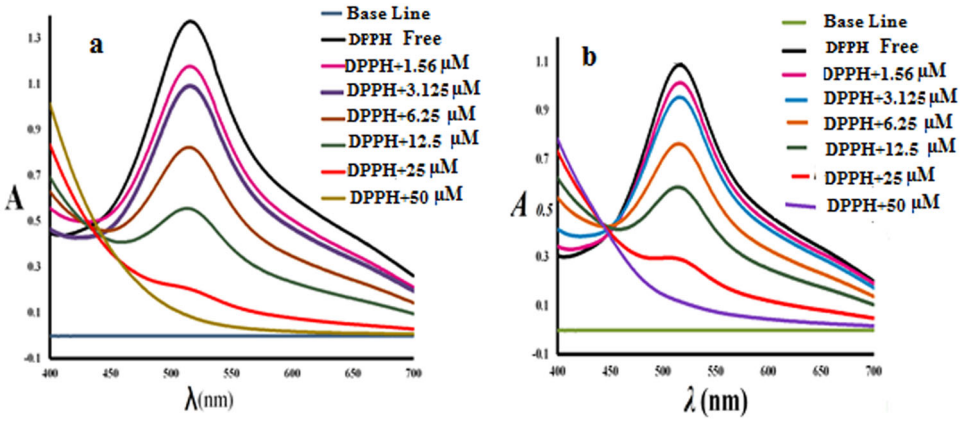

Figure 5. The UV-Vis absorption spectra of DPPH activity data for both the absence and presence of increasing concentration of **3** (A) and **2** (B).

The data show that **3** possesses the highest DPPH free radical scavenging ability (IC_{50} = 10 µg/mL) followed by **2** with IC_{50} value of 12 µg/mL and **1** having IC_{50} of 43 µg/mL.

3.5. Antibacterial activity

The synthesized compounds were also bioassayed against three bacterial strains, *Pseudomonas*, *S. aureus* and *E. coli*, using erythromycin as a positive control and methanol as a negative control. The activities were measured in the form of inhibition zone in centimeters. The antibacterial activities of all synthesized ligands and their complexes at different concentrations are shown in Table 3. Complexes **1**–**3** have significant activity against all of the tested bacterial strains and the values of inhibition zones are comparable to that of the standard drug. The antibacterial data demonstrate that fluorobenzoyl substituted thioureas have shown very good activity against *Pseudomonas* and *S. aureus* bacterial species. Similarly complexes **1** and **3** show good activity against the two bacterial strains whereas **2** having benzoyl substituent thiourea shows more activity against *E. coli*. Surprisingly thiourea derivatives show more antibacterial activity than **1**–**3**. It may be argued that triphenylphosphine reduces the toxicity but without affecting too much of their activity, retaining the activity at a reasonable level. Thus the data demonstrate that **1**–**3** have potential use in drug discovery processes and development.

3.6. Molecular docking analysis

In order to predict the best conformational position of **1**-**3** against *E. coli enoyl reductase* (PDB code: 1C14), the AutoDock tool was employed. Analysis of the generated docked complexes were done on the basis of the minimum energy values (kcal/mol) and binding interaction pattern (hydrogen/hydrophobic). Compounds **1**-**3** have good

Table 3. Antibacterial data for (I_1–I_3; **1–3**).

	Pseudomonas				*Staphylococcus aureus*				*E. coli*			
Compounds	Inhibition zones at different conc. (cm) 200 μg/ml	+ve Contl.* 400 μg/ml	–	−ve Contl.** –	Inhibition zones at different conc. (cm) 200 μg/ml	400 μg/ml	+ve Contl.* –	−ve Contl.** –	Inhibition zones at different conc. (cm) 200 μg/ml	400 μg/ml	+ve Contl.* –	−ve Contl.** –
I_1	2.5	4.5	4.0	1.9	3.5	5	6.3	2.3	3.9	5.0	6.0	2.3
I_2	3	3.9	5	2.0	2.9	3.9	4.5	2.3	2.9	3.5	4.1	2.1
I_3	2.5	4.0	5.0	2.0	3.8	5	6.0	2.0	3.8	5.1	6.0	2.0
1	2.0	3.8	4.5	1.8	2	4.2	4.5	1.8	2.1	4.0	4.7	1.8
2	2.0	3.0	4.0	2.0	4.0	4.5	5.4	2.1	4.0	4.7	5.0	2.0
3	2.8	4.0	4.5	2.0	1.5	4.2	5	2.2	1.7	4	5.1	2.2

*Erythromycin.
**Ethanol.

Table 4. Binding energies with *E. coli enoyl reductase* for **1–3**.

Compound	Binding affinity (kcal/mol)
1	−8.1
2	−6.4
3	−6.6

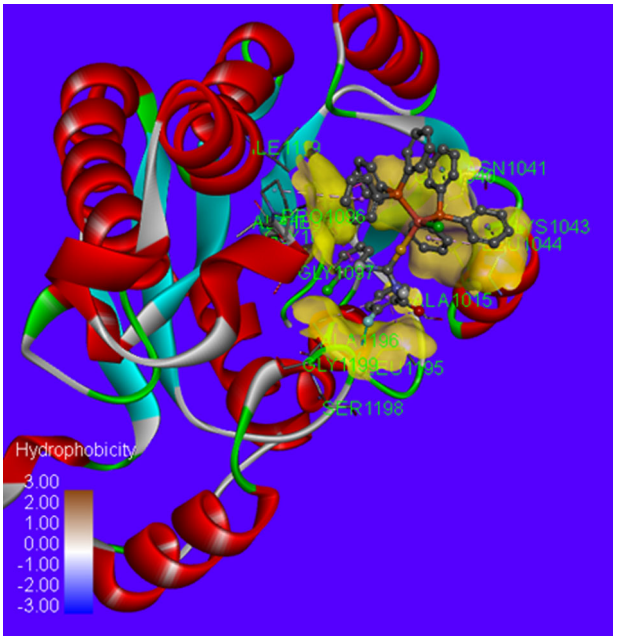

Figure 6. 3D depiction of docking for **1** in active site of *E. coli enoyl reductase*.

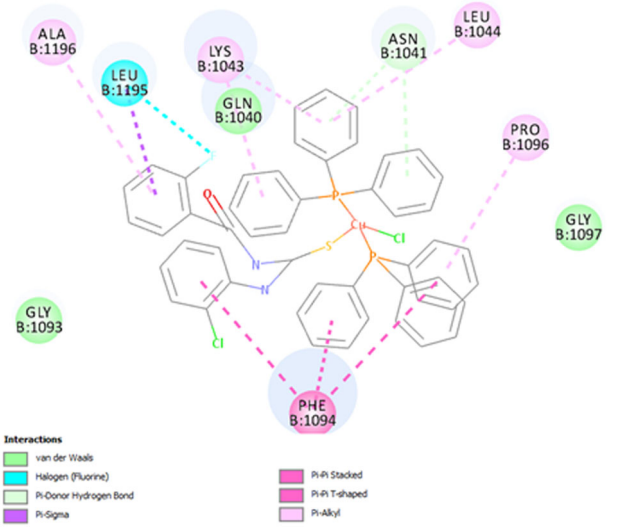

Figure 7. 2D depiction of docking for **1** in active site of *E. coli enoyl reductase*.

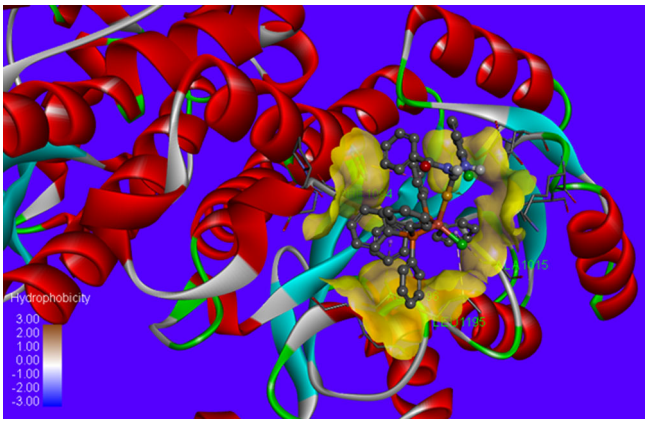

Figure 8. 3D depiction of docking for **2** in active site of *E. coli enoyl reductase*.

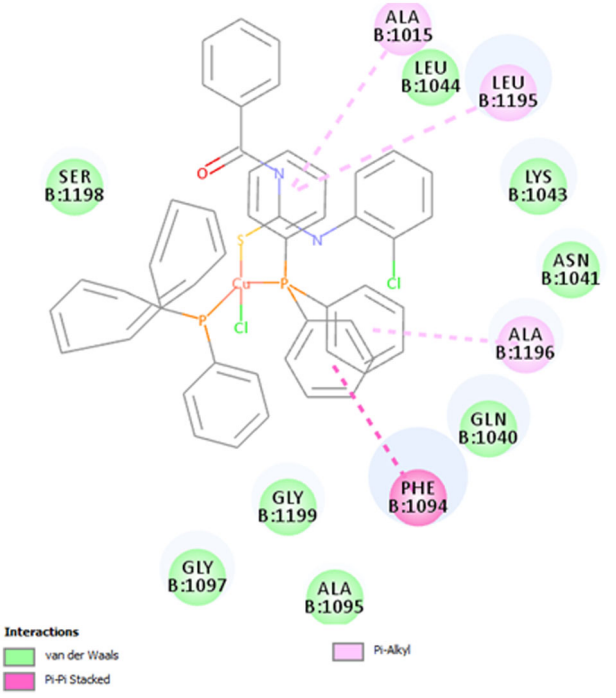

Figure 9. 2D depiction of docking for **2** in active site of *E. coli enoyl reductase*.

binding affinity and were observed to interact with the amino acid residues of the active pocket, however, **2** was found to have best fitting orientation in *E. coli enoyl reductase's* active pocket with binding affinity of −6.4 kcal/mol as revealed by the values (given) in Table 4. This pattern shows that major activity may be ascribed to the aromatic rings present in the thiourea moiety of **2** and are supposed to be mainly involved in hydrophobic interactions. The different interactions in the docked

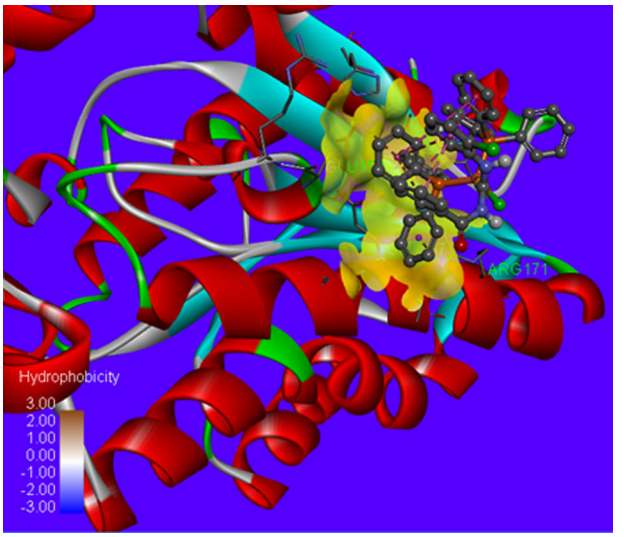

Figure 10. 3D depiction of docking for **3** in active site of *E. coli enoyl reductase*.

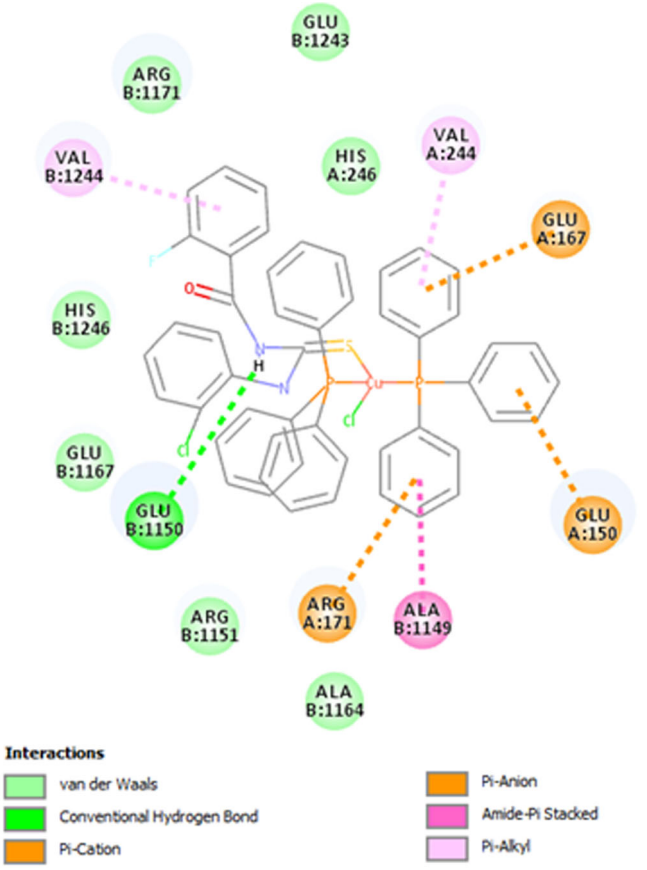

Figure 11. 2D depiction of docking for **3** in active site of *E. coli enoyl reductase*.

complexes have been delineated as 3D and 2D graphical depictions are shown in Figures 6–11.

4. Conclusion

Three substituted thioureas ($\mathbf{I_1}$–$\mathbf{I_3}$) and their Cu(I) complexes (**1**–**3**) were synthesized in the presence of triphenylphosphine as a mixed ligand. They were characterized by IR, NMR spectroscopy and single crystal X-ray diffraction. The X-ray data for **3** described that the central Cu of the complex is four coordinate with tetrahedral molecular geometry. They were screened for their antioxidant and antibacterial activities along with DNA binding studies and found some encouraging results. Complexes **1**–**3** interact electrostatically with the DNA back bone. The results of DPPH assay show that all compounds have very good free radical scavenging ability with the advantage of good antibacterial activity. The binding modes of the synthesized complexes with the specific target protein have also been explored by molecular docking studies.

Acknowledgements

Authors are thankful to HEC, Pakistan and Quaid-i-Azam University, Islamabad, Pakistan for their financial support.

Disclosure statement

There are no known conflicts of interest associated with this publication.

References

[1] H. Arslan, N. Külcü, U. Flörke. *Transition Met. Chem.*, **28**, 816 (2003).
[2] D.S. Mansuroglu, H. Arslan, U. Flörke, N. Külcü. *J. Coord. Chem.*, **61**, 3134 (2008).
[3] C.K. Ozer, H. Arslan, D. Vanderveer, G. Binzet. *J. Coord. Chem.*, **62**, 266 (2009).
[4] G. Binzet, H. Arslan, U. Flörke, N. Külcü, N. Duran. *J. Coord. Chem.*, **59**, 1395 (2006).
[5] D. Ugur, H. Arslan, N. Külcü. *Russ. J. Coord. Chem.* , **32**, 669 (2006).
[6] M. Emen, H. Arslan, N. Kulcu, U. Florke, N. Duran. *Pol. J. Chem.*, **79**, 1615 (2005).
[7] H. Arslan, U. Flörke, N. Külcü, M. Emen. *J. Coord. Chem.*, **59**, 223 (2006).
[8] W. Henderson, B.K. Nicholson, M.B. Dinger, R.L. Bennett. *Inorg. Chim. Acta*, **338**, 210 (2002).
[9] C. Sacht, M.S. Datt, S. Otto, A. Roodt. *J. Chem. Soc, Dalton Trans.* , 4579 (2000).
[10] M. Lipowska, B.L. Hayes, L. Hansen, A. Taylor, L.G. Marzilli. *Inorg. Chem.* , **35**, 4227 (1996).
[11] R.L. Zuckerman, R.G. Bergman. *Organometallics*, **19**, 4795 (2000).
[12] L. Barton, D.K. Srivastava. *J. Chem. Soc., Dalton Trans*, 1327 (1992).
[13] A. Saxena, R.D. Pike. *J. Chem. Crystallogr.* , **37**, 755 (2007).[
[14] X. Zhou, Y. Liang, F. Nan, Y. Ma. *Polyhedron*, **11**, 447 (1992).
[15] Y. Omote, R. Kobayashi, N. Sugiyama. *BCSJ.* , **46**, 2896 (1973).
[16] B.S. Garg, L. Kapur. *Inorg. Chim. Acta*, **170**, 177 (1990).
[17] S. Hussain, A. Badshah, B. Lal, R.A. Hussain, S. Ali, M.N. Tahir, A.A. Altaf. *J. Coord. Chem.*, **67**, 2148 (2014).
[18] F.A. French, E.J. Blanz. *Cancer Res.* , **25**, 1454 (1965).
[19] E.J. Blanz, F.A. French. *Cancer Res.* , **28**, 2419 (1968).
[20] K. Ramadas, G. Suresh, N. Janarthanan, S. Masilamani. *Pestic. Sci.* , **52**, 145 (1998).

[21] A.A. Aly, E.K. Ahmed, K.M. El-Mokadem, M. El-Amir, F. Hegazy. *J. Sulfur Chem.*, **28**, 73 (2007).
[22] M. Eweis, S. Elkholy, M. Elsabee. *Int. J. Biol. Macromol.* , **38**, 1(2006).
[23] B.R. Stern, M. Solioz, D. Krewski, P. Aggett, T.-C. Aw, S. Baker, K. Crump, M. Dourson, L. Haber, R. Hertzberg, C. Keen, B. Meek, L. Rudenko, R. Schoeny, W. Slob, T. Starr. *J Toxicol Environ Health B Crit Rev*, **10**, 157 (2007).
[24] S. Chandra, S. Raizada, M. Tyagi, P.K. Sharma. Spectrochim Acta A Mol Biomol Spectrosc, **69**, 816(2008). *Spectrochim. Acta*
[25] N. Metzler-Nolte, H. Kraatz. *Concepts and Models in Bioinorganic Chemistry*, Wiley-Vch New York (2006).
[26] I. Bertini, H.B. Gray, S.J. Lippard, J.S. Valentine. *Bioinorganic Chemistry*, University Science Books, Ausalito, CA (1994).
[27] J.F. Da Silva, R.J.P. Williams. *The Biological Chemistry of the Elements: The Inorganic Chemistry of Life*, Oxford University Press, Oxford, England (2001).
[28] M. Melník, M. Kabešová, M. Koman, L.U. Macášková, C.E. Holloway. *J. Coord. Chem.*, **50**, 177 (2000).
[29] E.A. Ambundo, M.-V. Deydier, A.J. Grall, N. Aguera-Vega, L.T. Dressel, T.H. Cooper, M.J. Heeg, L. Ochrymowycz, D. Rorabacher. *Inorg. Chem.* , **38**, 4233 (1999).
[30] N. Kitajima, Y. Moro-Oka. *Chem. Rev.* , **94**, 737 (1994).
[31] Y.F. Yuan, J.T. Wang, M.C. Gimeno, A. Laguna, P.G. Jones. *Inorg. Chim. Acta*, **324**, 309 (2001).
[32] Y.-M. Zhang, T.-B. Wei, L. Xian, L.-M. Gao. *Phosphorus, Sulfur Relat. Elem.*, **179**, 2007 (2004).
[33] Y.-M. Zhang, T.-B. Wei, X.-C. Wang, S.-Y. Yang. *ChemInform*, **29**, no (1998).
[34] Z. Weiqun, L. Baolong, Z. Liming, D. Jiangang, Z. Yong, L. Lude, Y. Xujie. *J. Mol. Struct.*, **690**, 145 (2004).
[35] M.K. Rauf, Imtiaz-Ud-Din, A. Badshah, M. Gielen, M. Ebihara, D. de Vos, S. Ahmed. *J. Inorg. Biochem.*, **103**, 1135 (2009).
[36] S.I. Khan, I.A. Khan, A. Badshah, F. Perveen Malik, S. Tabassum, I. Ullah, D. Zargarian, M. Khawar Rauf. *J. Coord. Chem.*, **71**, 4086 (2018).
[37] N. Gunasekaran, N. Bhuvanesh, R. Karvembu. *Polyhedron*, **122**, 39 (2017).
[38] A. Raheel, Imtiaz-Ud-Din, M.B. Taj, R. Ayub, M.N. Tahir, J. Raftery, M. Al-Shakban. *Chem. Select*, **4**, 8638 (2019).
[39] A. Raheel, Imtiaz-Ud-Din, M. Taj, M. Tahir, M. Al-Shakban. *Russ. J. Gen. Chem.*, **88**, 1508 (2018).
[40] A. Raheel, Imtiaz-Ud-Din, S. Andleeb, S. Ramadan, M.N. Tahir. *Appl. Organomet. Chem.*, **31**, e3632 (2017).
[41] M. Mehmood, Imtiaz-Ud-Din, M.N. Tahir, I. Haq, S.S. Zahra. *Inorg. Chim. Acta*, **486**, 387 (2019).
[42] T. Fatima, Imtiaz-Ud-Din, A. Akbar, M.S. Anwar, M.N. Tahir. *J. Mol. Struct.*, **1184**, 462 (2019).
[43] G.M. Morris, R. Huey, W. Lindstrom, M.F. Sanner, R.K. Belew, D.S. Goodsell, A.J. Olson. *J. Comput. Chem.* , **30**, 2785 (2009).
[44] N.M. O'Boyle, M. Banck, C.A. James, C. Morley, T. Vandermeersch. G.R. *Hutchison. J. Cheminformatics*, **3**, 33 (2011).
[45] H. Kalinowski, S. Berger, S. Braun. *Georg Thieme*, Verlag Stuttgart, New York (1961).
[46] A. Raheel, Imtiaz-Ud-Din, A. Badshah, M.K. Rauf, M.N. Tahir, K.M. Khan, A. Hameed, S. Andleeb. *J. Chem. Soc. Pak.*, **38**, 959 (2016).
[47] M.Z. Zubir, N.S. Jamaludin, S.N. Halim. *J. Mol. Struct.*, **1193**, 141 (2019).
[48] R.A. Hussain, A. Badshah, M.N. Tahir, B. Lal, I.A. Khan. *Aust. J. Chem.* , **66**, 626(2013).